Journal of Solid State Chemistry 184 (2011) 171–176

Contents lists available at ScienceDirect

Journal of Solid State Chemistry

journal homepage: www.elsevier.com/locate/jssc

Phosphate-intercalated Ca–Fe-layered double hydroxides: Crystal structure, bonding character, and release kinetics of phosphate

Myong A. Woo, Tae Woo Kim, Mi-Jeong Paek, Hyung-Wook Ha, Jin-Ho Choy, Seong-Ju Hwang *

Center for Intelligent Nano-Bio Materials (CINBM), Department of Chemistry and Nano Sciences, Ewha Womans University, Seoul 120-750, Republic of Korea

ARTICLE INFO

Article history:
Received 20 July 2010
Received in revised form
30 September 2010
Accepted 7 November 2010
Available online 13 November 2010

Keywords:
Layered double hydroxide
Phosphate intercalation
Slow release
Acid neutralization
Release kinetics

ABSTRACT

The nitrate-form of Ca–Fe-layered double hydroxide (Ca–Fe-LDH) was synthesized via co-precipitation method, and its phosphate-intercalates were prepared by ion-exchange reaction. According to X-ray diffraction analysis, the Ca–Fe-LDH–NO_3^- compound and its $H_2PO_4^-$-intercalate showed hexagonal layered structures, whereas the ion-exchange reaction with HPO_4^{2-} caused a frustration of the layer ordering of LDH. Fe *K*-edge X-ray absorption spectroscopy clearly demonstrated that the Ca–Fe-LDH lattice with trivalent iron ions was well-maintained after the ion-exchange with HPO_4^{2-} and $H_2PO_4^-$. Under acidic conditions, phosphate ions were slowly released from the Ca–Fe-LDH lattice and the simultaneous release of hydroxide caused the neutralization of acidic media. Fitting analysis based on kinetic models indicated a heterogeneous diffusion process of phosphates and a distinct dependence of release rate on the charge of phosphates. This study strongly suggested that Ca–Fe-LDH is applicable as bifunctional vector for slow release of phosphate fertilizer and for the neutralization of acid soil.

1. Introduction

Over recent decades, layered double hydroxides (LDHs) have received primary attention as useful delivery vector for diverse biomolecules and drug molecules because of its unique ability to immobilize anionic species in the interlayer space [1–6]. This material is a class of lamellar compound that consists of positively charged brucite-type host layers and hydrated exchangeable anions located in the interlayer gallery. The chemical composition of LDHs can be expressed by the general formula $[M^{2+}_{1-x}M^{3+}_x(OH)_2]^{x+}[A^{n-}_{x/n}]^{x-}\cdot zH_2O$, where M^{2+}, M^{3+}, and A^{n-} denote divalent metal ions (e.g., Ca^{2+}, Mg^{2+}, Zn^{2+}, Ni^{2+}, Mn^{2+}, Co^{2+}, Fe^{2+}, Cu^{2+}, etc.), and trivalent metal ions (e.g., Fe^{3+}, Al^{3+}, Cr^{3+}, Mn^{3+}, Ga^{3+}, Co^{3+}, Ni^{3+}, etc.), and interlayer anions, respectively. Some M^{2+} metal cations are partially substituted by M^{3+} cations, leading to the generation of a positively charged layer. As a consequence, anions can be intercalated in the interlayer space of the LDH to maintain charge neutrality. Because of its monovalent charge state, the nitrate ions in the interlayer space of the LDHs can be readily exchanged with other anions [7,8]. Hence, the nitrate-form of LDH has a great potential as an efficient reservoir for diverse organic and biomolecular anions such as DNA [1], amino acids [2], anionic polymers [3], or drugs [4–6]. Most functionalities of the LDH originate from the release of guest species intercalated. Hence, it is of high importance to understand the release kinetics of guest species immobilized in the LDH lattice in optimizing the functionalities of LDH-based materials. There would be many factors affecting the release rate of the guest species including a chemical interaction between host and guest, the crystal size of the intercalation compound, the chemical stability of intercalation structure, etc. Considering the polyprotic nature of phosphate anions ($H_2PO_4^-$, HPO_4^{2-}, and PO_4^{3-}), the intercalation of phosphate ions into the LDH can provide useful opportunity to elucidate the effect of guest–host interaction on the deintercalation behavior of the guest species. Moreover, taking into consideration the role of phosphates as fertilizer, the phosphate-intercalated LDH materials are expected to act as an effective delivery vector for the slow release of fertilizer; in acidic conditions, the basic LDH lattice can be slowly decomposed, leading to the slow release of the intercalated phosphate components. The simultaneous evolution of hydroxide ions from the LDH lattice would ameliorate the acidification of soil caused by chemical fertilizer and/or acid rain [9].

In the present study, the nitrate-form of $[Ca^{2+}_{1-x}Fe^{3+}_x(OH)_2]^{x+}[NO_{3\,x}^-]^{x-}\cdot zH_2O$ (hereafter denoted it as Ca–Fe-LDH–NO_3^-) and its phosphate-intercalates were synthesized by co-precipitation and subsequent ion-exchange reactions, respectively. Taking into account the possible environmental and agricultural use of LDH, Ca–Fe-LDH was selected as a host material because of its environmentally benign chemical composition. The crystal structure, morphology, and chemical bonding nature of the obtained Ca–Fe-LDH-based materials were systematically characterized with the combination of diffraction, microscopic, and spectroscopic tools. In addition, the release kinetics of intercalated phosphate ions was investigated together with the accompanying variation of pH during the dissolution of the host LDH lattice.

* Corresponding author. Fax: +82 2 3277 3419.
E-mail address: hwangsju@ewha.ac.kr (S.-J. Hwang).

0022-4596/$ - see front matter © 2010 Elsevier Inc. All rights reserved.
doi:10.1016/j.jssc.2010.11.003

2. Experimental

2.1. Synthesis

For the preparation of pristine Ca–Fe-LDH–NO_3^-, $Ca(NO_3)_2 \cdot 4H_2O$ and $Fe(NO_3)_3 \cdot 9H_2O$ were dissolved in deionized water to give final concentrations of 30 and 10 mM, respectively. Then, the mixed solution was magnetically stirred at room temperature under a nitrogen atmosphere at a pH of 12 ± 1. The pH of the reactant solution was adjusted by adding 1 M NaOH solution. After the reaction had proceeded for 2 days, the precipitates were collected by centrifugation, washed with absolute ethanol, and dried under vacuum at room temperature. The intercalation of dihydrogen phosphate or hydrogen phosphate anions into the Ca–Fe-LDH was achieved by reacting 100 mg of Ca–Fe-LDH–NO_3^- powder with 100 mL of 0.1 M aqueous solution of KH_2PO_4 or K_2HPO_4 at room temperature under vigorous stirring [10]. The initial pH of the reactant KH_2PO_4 and K_2HPO_4 solution was measured as ~4.5 and ~9.1, respectively, in which phosphate ions mainly exist as $H_2PO_4^-$ and HPO_4^{2-}. The ion-exchange reactions proceeded for 2 days. The resultant precipitates were washed with deionized water and dried at room temperature.

2.2. Characterization

The crystal structures of the pristine Ca–Fe-LDH–NO_3^- and its phosphate-intercalates were studied by powder X-ray diffraction (XRD, Rigaku, $\lambda = 1.5418$ Å). The crystal morphologies of these materials were probed by field emission-scanning electron microscopy (FE-SEM, Jeol JSM-6700F). The local crystal structure and chemical composition of the phosphate-intercalated Ca–Fe-LDH were examined with transmission electron microscopy-selected area electron diffraction (TEM-SAED, JEOL JEM-2100F, 200 kV) installed energy dispersive spectrometry (EDS) machine. The chemical compositions and thermal behaviors of the present LDH materials were investigated by performing electron probe microanalysis (EPMA, Jeol JXA-8100) and thermogravimetric analysis (TGA, Rigaku TAS-100), respectively. Fourier-transform infrared (FT-IR) spectra in the frequency range of $400 - 4000\ cm^{-1}$ were recorded on a Jasco FT/IR-6100 FT spectrometer. Before the measurements, the samples were finely pulverized, mixed with KBr, and pressed to translucent pellets. X-ray absorption near-edge structure (XANES) experiments were carried out at the Fe *K*-edge with the extended X-ray absorption fine structure (EXAFS) facility installed at beam line 7C at the Pohang Accelerator Laboratory (PAL) in Korea. The present XANES data were collected from the thin layer of powder samples deposited on transparent adhesive tapes in a transmission mode using gas-ionization detectors. The measurements were carried out at room temperature with a Si(111) single crystal monochromator. No focusing mirror was used. All of the present spectra were carefully calibrated by simultaneously measuring iron metal foil.

2.3. Measurements of phosphate release rate and acid neutralization

The release behavior of the phosphate ions stabilized in the LDH lattice was analyzed in weakly acidic media (pH = 5.2). Phosphate-intercalated Ca–Fe-LDH powder (0.2 g/L) was dispersed in the buffer solution at pH = 5.2 or in aqueous HCl solution at the same pH, and stirred at 20 °C at a rate of 200 rpm. The amount of phosphate ions released from the Ca–Fe-LDH–phosphate was estimated with ion chromatography (IC). In order to understand the kinetics for the release behavior of phosphate ions, we tried to fit the measured data to several kinetic models [4–6,11].

A first-order rate model can describe the ion-exchange reaction or release process. This model is expressed as follows:

$$\ln(C_t/C_0) = -k_d t \quad (1)$$

In this equation, C_0 is the total amount of intercalated phosphates in the LDH lattice at zero time of release, C_t is the total amount of released phosphates after the period t, and k_d is the apparent release rate constant.

A parabolic diffusion equation is appropriate to describe diffusion-controlled phenomena in clays [4]. The parabolic diffusion model is expressed as follows:

$$(1 - C_t/C_0)/t = k_d t^{-0.5} + a \quad (2)$$

In this equation, a is a constant and k_d is the overall diffusion constant for release.

A modified Freundlich model is applicable for experimental data on ion-exchange or adsorption with clays [4]. This model is described as follows:

$$C_0 - C_t = k_d C_0 t^a \quad (3)$$

In this equation, k_d is the release rate coefficient and a is a constant.

During the release test of phosphate ions in the aqueous HCl solution with a starting pH of 5.2, the variation of the solution pH was also monitored by pH meter.

3. Results and discussion

3.1. Powder XRD and FE-SEM analyses

The powder XRD patterns of the pristine Ca–Fe-LDH–NO_3^- and its phosphate-intercalates are plotted in the left panel of Fig. 1. The Ca–Fe-LDH–NO_3^- exhibits a series of well-defined (00*l*) Bragg reflections without any impurity peaks, clearly demonstrating the formation of single-phase LDHs with a hexagonal layered structure [12,13]. After the ion-exchange with $H_2PO_4^-$, overall XRD features characteristic of a layered LDH lattice were well-maintained with slight shifts toward high angle side, suggesting the decrease of basal spacing. According to least squares fitting analysis, the lattice parameters were determined to be $a = 0.589$

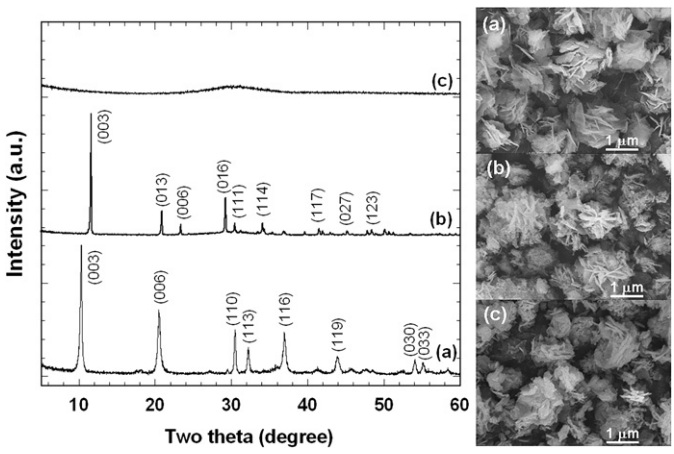

Fig. 1. (Left) Powder XRD and (right) FE-SEM data of (a) Ca–Fe-LDH–NO_3^- and its intercalates of (b) $H_2PO_4^-$ and (c) HPO_4^{2-}.

and $c=2.611$ nm for the pristine Ca–Fe-LDH–NO_3^- and $a=0.596$ and $c=2.255$ nm for Ca–Fe-LDH–$H_2PO_4^-$, respectively.

This finding is contrasted with the previous studies showing no change or slight increase in the basal spacing of LDH upon the exchange of nitrate with phosphate [14–16]. From the TGA analysis, an exchange with phosphate ions decreases the water content of the nitrate-form of Ca–Fe-LDH (see Fig. 2). This would be responsible for the observed decrease of basal spacing upon ion-exchange. In contrast to the intercalation of $H_2PO_4^-$, the ion-exchange reaction with higher-valence HPO_4^{2-} anion suppresses most Bragg reflections of the LDH lattice, including intense (00*l*) peaks. This observation strongly suggests that the layer-by-layer ordering of the LDH lattice along the *c*-axis becomes significantly impeded after the ion-exchange by this higher-valence anion. This would be attributed to charge difference between NO_3^- and HPO_4^{2-}, resulting in a significant mismatch in charge density between the Ca–Fe-LDH layers and exchanged phosphate anions and eventually in the disordering of interstratified structures. To probe the maintenance of LDH layer after the ion-exchange with HPO_4^{2-}, we carried out TEM-SAED analysis for this HPO_4^{2-}-intercalated Ca–Fe-LDH. A clear hexagonal SAED pattern corresponding to hexagonal LDH lattice can be observed for the HPO_4^{2-} intercalated Ca–Fe-LDH, underscoring the maintenance of LDH layers in this compound (see *Supplementary data*). Hence, the observed X-ray amorphous nature of this material is due to the disordered stacking of exfoliated nanosheets, not to the decomposition of the LDH lattice. Similar amorphous XRD patterns were observed for the disordered stacking of exfoliated layered metal oxide nanosheets [17].

The right panel of Fig. 1 shows the FE-SEM images of the pristine Ca–Fe-LDH–NO_3^- and its phosphate-intercalates. The pristine Ca–Fe-LDH–NO_3^- displays hexagonal plate-like morphology, with a primary particle size of ~1–2 μm. The plate-like morphology remains unchanged after the ion-exchange of nitrate with phosphates, but the particle size becomes somewhat smaller, which would be attributable to the crystal strain caused by the ion-exchange process. It is worthwhile to mention that, even though the ion-exchange with HPO_4^{2-} suppresses the XRD peaks of the pristine Ca–Fe-LDH–NO_3^- (Fig. 1), the plate-like morphology of the LDH crystallites is well-maintained after the incorporation of HPO_4^{2-}. This can be interpreted as indirect evidence for the maintenance of the LDH structures upon the exchange with divalent hydrogen phosphate ions. Conversely, we tried the exchange of interlayer NO_3^- anions with PO_4^{3-} anions through a reaction between the Ca–Fe-LDH–NO_3^- powder and the aqueous solution of K_3PO_4. But this reaction caused the decomposition of the LDH lattice, resulting in the formation of $Ca_5(PO_4)_3OH$ phase. In this case, the plate-like morphology of the pristine Ca–Fe-LDH–NO_3^- is completely destroyed after the reaction with PO_4^{3-} ions.

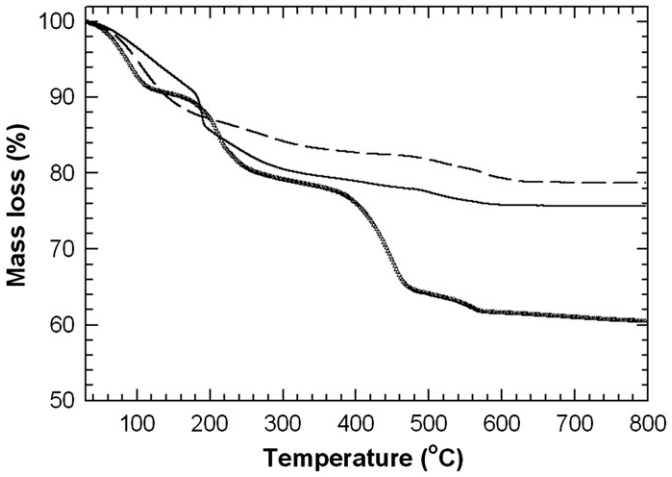

Fig. 2. TGA curves for Ca–Fe-LDH–NO_3^- (triangles), Ca–Fe-LDH–$H_2PO_4^-$ (solid lines), and Ca–Fe-LDH–HPO_4^{2-} (dashed lines).

3.2. TGA and elemental analysis

The thermal behaviors of the pristine Ca–Fe-LDH–NO_3^- and its phosphate-intercalates were examined using TGA. As plotted in Fig. 2, all the present materials exhibit notable mass losses in the temperature range 100–400 °C, corresponding to the evaporation of water molecules and dehydroxylation of the LDH lattice. The mass loss in this temperature region is larger for the pristine compound than for the phosphate-intercalates, indicating the higher water content of the former. The pristine Ca–Fe-LDH–NO_3^- compound shows additional notable mass loss around 400 − 500 °C, which is related to the evaporation of interlayer nitrate ions. Conversely, this nitrate-related mass loss is absent in the TGA curves of the phosphate-intercalates, which confirms the complete exchange of nitrate with phosphate.

According to the EPMA results, the pristine Ca–Fe-LDH–NO_3^- showed a Ca/Fe ratio of ~1.3, and the ion-exchange reaction with phosphate has little influence on the Ca/Fe ratio of the LDH lattice, strongly suggesting no preferential dissolution of Ca or Fe ions during the reaction (see *Supplementary data*). Both the phosphate-intercalated Ca–Fe-LDHs contain a large amount of phosphate anions with the P/Fe ratio of ~1.5 − 2.5, underscoring the successful immobilization of phosphate ions in the LDH lattice. In comparison with higher-valence HPO_4^{2-} ion, a larger amount of monovalent $H_2PO_4^-$ ions can be intercalated into the Ca–Fe-LDH lattice. This could be well-understood in terms of charge neutrality between positively charged Ca–Fe-LDH host layers and phosphate guest anions. It should be noted that the P/Fe ratios of the ion-exchange products are somewhat greater than the theoretical amount of exchangeable nitrate ions, even though the ion-exchanged samples were thoroughly washed with water. This suggests that excess phosphate ions are adsorbed on the surface of LDH crystallites via the formation of anchoring bonds.

3.3. FT-IR spectroscopy

The ion-exchange of interlayer nitrate ions with phosphate ions was evidenced by the results of FT-IR spectroscopy. Fig. 3 shows the FT-IR spectra of the pristine Ca–Fe-LDH–NO_3^- and its phosphate-intercalates. The broad absorption band at ~3400 cm^{-1} is assigned as the stretching of hydroxide groups in the LDH layer and/or in the intercalated water molecules [12]. The strong absorption band at 1380 cm^{-1} is attributed to the ν_3 (NO_3^-) vibration, whereas the weak bands at ~825 and ~665 cm^{-1} correspond to the ν_1 and ν_4 vibrations, respectively, of the nitrate groups [12]. After the ion-exchange reaction, these nitrate-related IR bands disappeared but the phosphate-related bands became discernible at around 900 − 1200 cm^{-1}. The present FT-IR results provide strong evidence for the complete replacement of the interlayer nitrate ions with phosphate ions. The compete replacement of nitrate ions with phosphate ions was confirmed by TEM-EDS elemental line profile analysis showing the negligible content of nitrogen elements in the phosphate-intercalates (see *Supplementary data*).

3.4. Fe K-edge XANES analysis

The oxidation state and local symmetry of iron ions in the present Ca–Fe-LDH-based materials were investigated using Fe *K*-edge XANES analysis. As plotted in Fig. 4, the edge position of the pristine Ca–Fe-LDH–NO_3^- is nearly the same as that of the reference

α-Fe_2O_3, indicating the trivalent oxidation state of the iron ions. Before and after the ion-exchange reaction with phosphates, there was no marked change in edge position, indicative of the maintained trivalent Fe oxidation state. As can be clearly seen from the right panel of Fig. 4, all of the present LDHs exhibit the pre-edge peak P at ~7115 eV, which corresponds to the $1s \rightarrow 3d$ transition. Although this transition with $\Delta l = 2$ is forbidden by the electronic dipolar selection rule, the pre-edge peak obtains significant spectral weight for the tetrahedral iron through the mixing of 4*p* and 3*d* states [18]. On the contrary, this peak is very weak for a centrosymmetric octahedral symmetry, in which the mixing between 4*p* and 3*d* orbitals is negligible. Among the materials under investigation, this peak shows the largest spectral weight for the reference Fe_3O_4 with the spinel structure, because one-third of the iron ions in this material have tetrahedral symmetry. The phosphate-intercalated Ca–Fe-LDH materials as well as the pristine Ca–Fe-LDH–NO_3^- exhibit only a weak pre-edge peak at the same energy. This provides strong evidence for the maintenance of octahedral symmetry and the trivalent oxidation state of iron ions before and after the ion-exchange reaction with phosphate ions. In the main-edge region, there are several peaks, denoted A and B corresponding to dipole-allowed $1s \rightarrow 4p$ transitions [18]. With the ion-exchange process, the resonance peak B of the pristine material becomes somewhat broader, which reflects the depression of crystallinity and/or the decrease in particle size caused by the intercalation of phosphates.

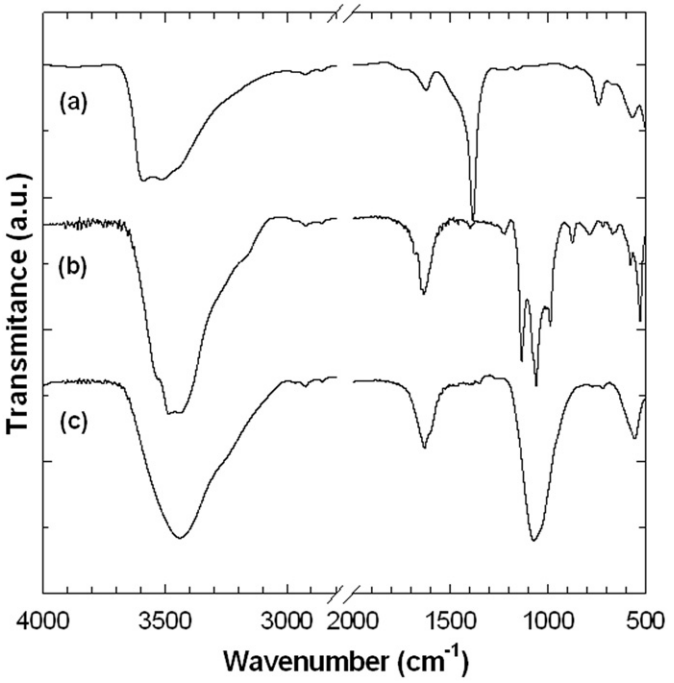

Fig. 3. FT-IR spectra of (a) Ca–Fe-LDH–NO_3^-, (b) Ca–Fe-LDH–$H_2PO_4^-$, and (c) Ca–Fe-LDH–HPO_4^{2-}.

3.5. Release behavior and acid neutralization

The release behavior of the phosphate ions intercalated in the Ca–Fe-LDH lattice was examined by monitoring the concentration of phosphate released as a function of reaction time. To rule out the effect of pH change during the release test, we adapted a weakly acidic buffer solution, with pH = 5.2, as a reaction medium. The solution pH was adjusted to the pH of natural water. In these conditions, the Ca–Fe-LDH lattice can be continuously decomposed without notable change in pH, and hence the intercalated phosphate can be effectively released. It is worthwhile to mention that the present test condition with buffered solution is ideal but different from the outdoor condition where the LDH-based vectors will be practically used. In the practical condition, the LDH-based materials will contact with non-buffered water, not with buffer solution. This leads to slower release of phosphate ions from the LDH lattice because of the pH increase upon the dissolution of the LDH.

The evolution of phosphate ions from the LDH lattice is plotted in Fig. 5 as a function of reaction time. Both the phosphate-intercalated Ca–Fe-LDH compounds show a rapid release of

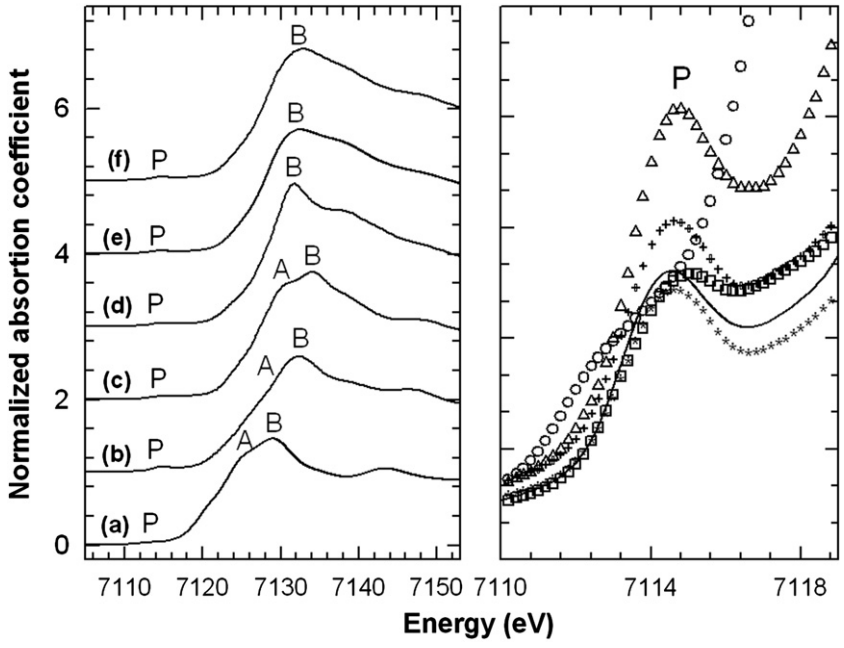

Fig. 4. (Left) Fe *K*-edge XANES spectra and (right) expanded view for pre-edge spectra for (a) FeO (circles), (b) Fe_3O_4 (triangles), (c) α-Fe_2O_3 (squares), (d) the pristine Ca–Fe-LDH–NO_3^- (solid lines) and its ion-exchange derivatives by (e) $H_2PO_4^-$ (crosses) and (f) HPO_4^{2-} (asterisks).

phosphates near the surface at the initial stage, followed by a slower release of the guest molecules. Such a release profile is characteristic of a diffusion-controlled release process [4,5].

To obtain more detailed information about the release mechanism of the phosphate ions, we tried to fit the observed release data to several kinetic models [4,6], as plotted in Fig. 6. The obtained rate constants and the r^2 values of the best fits are listed in Table 1. Among the present models, the modified Freundlich model gave reasonable r^2 values – about 0.99 – whereas poorer r^2 values were obtained for the first-order kinetic model and the parabolic diffusion model. The modified Freundlich model represents the release profiles from the flat surface with the heterogeneous sites by a diffusion process [5]. This result suggests that the release of the intercalated phosphate from the LDH lattice is a kind of heterogeneous diffusion processes, which would be related to the dissolution of the LDH layer that produces many heterogeneous sites. From the calculation with the modified Freundlich model, the rate coefficient (k_d) of the phosphate release for the Ca–Fe-LDH–phosphate intercalates was determined to be $\sim 0.6834-0.7614$. The Ca–Fe-LDH–$H_2PO_4^-$ showed a slower rate constant than the Ca–Fe-LDH–HPO_4^{2-}.

The diffusion rate of the intercalated species can be affected by several factors, such as the particle size of the intercalation compound, chemical interactions between host and guest, and the packing pattern of the guest species [5]. As found from FE-SEM images (the right panel of Fig. 1), the $H_2PO_4^-$-intercalation compound has a larger particle size than the other intercalate. Taking into account the fact that the release of intercalated phosphate in acidic conditions mainly occurs by dissolution of the host LDH lattice, the particle size of the phosphate-intercalates will play a main role in determining the rate constant of phosphate release. The Ca–Fe-LDH–$H_2PO_4^-$ intercalate also showed much higher structural order than the Ca–Fe-LDH–HPO_4^{2-} intercalate, as found from XRD analysis (the left panel of Fig. 1). The well-ordered crystal structure provides higher lattice energy stabilization and is therefore more resistant to chemical corrosion and/or the deintercalation of guest species. Judging from the charge of guest phosphate species, an interaction between host and guest would be expected to be larger for the higher-valence guest HPO_4^{2-} than for $H_2PO_4^-$. In this case, the former ion would be slowly released from its chemical interaction with the positively charged LDH lattice. However, this supposition is not compatible with the observed order of the rate constant, confirming that the release of the phosphate ions is mainly due to the dissolution of the LDH lattice rather than to the deintercalation of the guest ions.

We also examined the pH variations in the aqueous media caused by the decomposition of the LDH lattice and the simultaneous release of hydroxide ions. In this experiment, we used non-buffered HCl solution to adjust the initial pH of the reaction media to 5.2. After the immersion of the phosphate-intercalated Ca–Fe-LDH (0.1 g) into aqueous solution (100 mL), the initial pH of 5.2 is increased to $\sim$6.6 for $H_2PO_4^-$ and $\sim$8.4 for HPO_4^{2-}. Such a pH change is surely due to the release of hydroxide ions from the LDH lattice, highlighting the role of the host Ca–Fe-LDH lattice for the neutralization of acid soil. The lower pH obtained with $H_2PO_4^-$-intercalate would be related to the deprotonation of released dihydrogen phosphate ions.

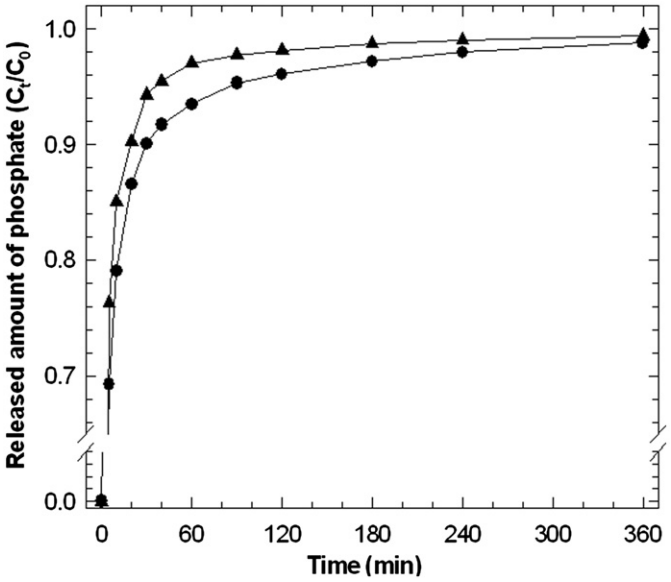

Fig. 5. Release profiles of phosphate ions from Ca–Fe-LDH–$H_2PO_4^-$ (circles) and Ca–Fe-LDH–HPO_4^{2-} (triangles) in a buffer solution with the pH of 5.2.

Table 1
Rate constants and r^2 coefficients obtained from fitting analyses based on several kinetic equations.

Kinetic equation	Ca–Fe-LDH–$H_2PO_4^-$	Ca–Fe-LDH–HPO_4^{2-}
First-order model	k_d=0.1903 r^2=0.944	k_d=0.251 r^2=0.974
Parabolic diffusion model	k_d=0.3156 a=−0.0262 r^2=0.966	k_d=0.3454 a=−0.0296 r^2=0.956
Modified Freundlich model	k_d=0.6834 a=0.0694 r^2=0.986	k_d=0.7614 a=0.0516 r^2=0.989

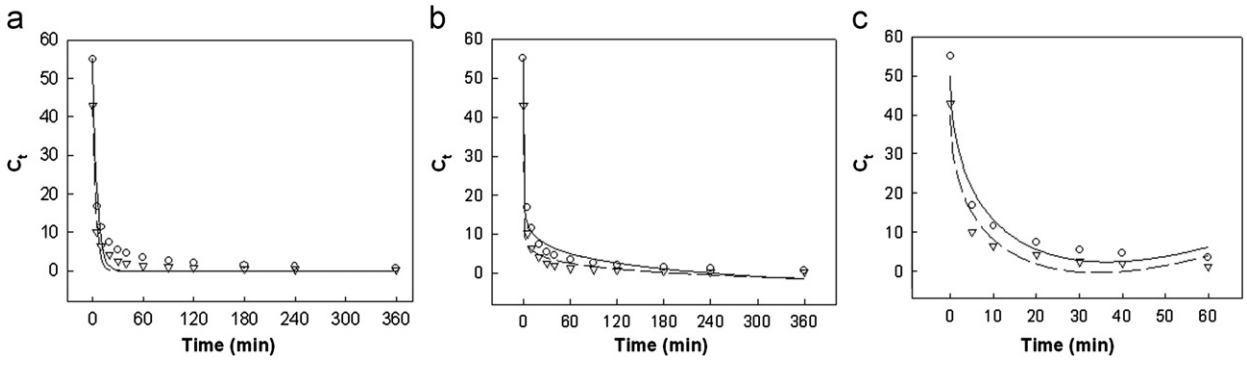

Fig. 6. Release profiles of phosphate ions (symbols) and their fits (lines) based on kinetic equations of (a) first-order kinetic model, (b) parabolic diffusion model, and (c) modified Freundlich model for the release of phosphates ions from Ca–Fe-LDH–$H_2PO_4^-$ (circles/solid lines) and Ca–Fe-LDH–HPO_4^{2-} (triangles/dashed lines).

With this non-buffered acidic solution, we also monitored the release behavior of the intercalated phosphate ions (see *Supplementary data*). As expected, both of the Ca–Fe-LDH–phosphate materials show much slower release of phosphate ions compared with the results with the buffer solution (Fig. 5). This observation can be well explained in terms of the fact that the increase in pH during the test retards the dissolution of the host LDH lattice, and hence suspends the release of the intercalated phosphate ions. In outdoor condition where the present LDH-based materials will be practically used, these materials will contact with non-buffered water, not with buffer solution. This leads to a slower release of phosphate ions from the LDH lattice.

4. Conclusions

In the present work, it is found that the charge of guest phosphate ions affects significantly the crystal structure and chemical bonding nature of the Ca–Fe-LDH-based intercalation compounds and the release rate of intercalated phosphate species. Under acidic conditions, phosphate ions are slowly released from the Ca–Fe-LDH lattice and the simultaneous dissolution of the LDH lattice makes possible the neutralization of acidic media. According to fitting analysis based on several kinetic models, intercalated phosphate ions show slow release via a heterogeneous diffusion process and there is a distinct dependence of release rate on the charge of phosphate ions. The slower release of guest species is obtained for the monovalent $H_2PO_4^-$ ions, indicating that the well-ordered crystal structure of the intercalation compound is important in optimizing the release rate of the guest species. Our next project, currently underway, is the further control of the release rate of immobilized phosphate species via surface coating and/or size tuning of the host Ca–Fe-LDH crystals.

Supplementary data

Lattice parameters and elemental analysis results, and the release profiles of phosphate for Ca–Fe-LDH–phosphates in non-buffered solution. SAED pattern of Ca–Fe-LDH–HPO_4^{2-} and TEM-EDS elemental line profile analysis of Ca–Fe-LDH–phosphates.

Acknowledgments

This work was supported by Korea Ministry of Environment as "Converging Technology Project" (191-101-001), the Korea Research Foundation Grant funded by the Korean Government (KRF-2008-313-C00442) and the outcome of a Manpower Development Program for Energy & Resources supported by the Ministry of Knowledge and Economy (MKE), and supported by National Research Foundation of Korea Grant funded by the Korean Government (20090063005). Pohang Accelerator Laboratory (PAL) were supported in part by MOST and POSTECH.

Appendix A. Supporting information

Supplementary data associated with this article can be found in the online version at doi:10.1016/j.jssc.2010.11.003.

References

[1] S.Y. Kwak, Y.J. Jeong, J.S. Park, J.H. Choy, Solid State Ionics 151 (2002) 229–234.
[2] T. Hibino, Chem. Mater. 16 (2004) 5482–5488.
[3] C. Manzi-Nshuti, D. Wang, J.M. Hossenlopp, C.A. Wilkie, J. Mater. Chem. 18 (2008) 3091–3102.
[4] J.H. Yang, Y.S. Han, M. Park, T. Park, S.J. Hwang, J.H. Choy, Chem. Mater. 19 (2007) 2679–2685.
[5] A.I. Khan, A. Ragavan, B. Fong, C. Markland, M. O'Brien, T.G. Dunbar, G.R. Williams, D. O'Hare, Ind. Eng. Chem. Res. 48 (2009) 10196–10205.
[6] H.S. Panda, R. Srivastava, D. Bahadur, J. Phys. Chem. B 113 (2009) 15090–15100.
[7] A.V. Radha, P. Vishnu Kamath, C. Shivakumara, Solid State Sci. 7 (2005) 1180–1187.
[8] T. Hibino, A. Tsunashima, Chem. Mater. 9 (1997) 2082–2089.
[9] D.L. Sparks, Environmental Soil Chemistry, 2nd ed., Academic Press, UK, 2003.
[10] We tried the exchange of interlayer NO_3^- anions with PO_4^{3-} anions by reacting the Ca–Fe-LDH–NO_3^- powder with the aqueous solution of K_3PO_4. But this reaction caused the decomposition of the LDH lattice, resulting in the formation of $Ca_5(PO_4)_3OH$ phase with non-layered crystal morphology.
[11] D.L. Sparks, Kinetics of Soil Chemical Processes, Academic Press, San Diego, CA, 1989.
[12] G.R. Williams, D. O'Hare, Solid State Sci. 8 (2006) 971–980.
[13] I. Rousselot, C. Taviot-Guého, F. Leroux, P. Léone, P. Palvadeau, J.P. Besse, J. Solid State Chem. 167 (2002) 137–144.
[14] Y. Du, N. Rees, D. O'Hare, Dalton Trans. (2009) 8197–8202.
[15] G.P. Gillman, M.A. Noble, M.D. Raven, Appl. Clay Sci. 38 (2008) 179–186.
[16] R. Segni, L. Vieille, F. Leroux, C. Taviot-Guého, J. Phys. Chem. Solids 67 (2006) 1037–1042.
[17] Y. Omomo, T. Sasaki, L.Z. Wang, M. Watanabe, J. Am. Chem. Soc. 125 (2003) 3568–3575.
[18] T.W. Kim, H.W. Ha, M.J. Paek, I.H. Paek, S.H. Hyun, J.H. Choy, S.J. Hwang, J. Phys. Chem. C 112 (2008) 14853–14862.